Title: Development, identification and validation of a mathematical model of anaerobic digestion of sewage sludge focusing on H_2S formation and transfer

Author: F. Carrera-Chapela A. Donoso-Bravo D. Jeison I. Díaz J.A. Gonzalez G. Ruiz-Filippi

PII: S1369-703X(16)30079-1
DOI: http://dx.doi.org/doi:10.1016/j.bej.2016.03.008
Reference: BEJ 6426

To appear in: *Biochemical Engineering Journal*

Received date: 30-11-2015
Accepted date: 18-3-2016

Please cite this article as: F. Carrera-Chapela, A. Donoso-Bravo, D. Jeison, I. Díaz, J.A. Gonzalez, G. Ruiz-Filippi, Development, identification and validation of a mathematical model of anaerobic digestion of sewage sludge focusing on H_2S formation and transfer, <*![CDATA[Biochemical Engineering Journal]]*> (2016), http://dx.doi.org/10.1016/j.bej.2016.03.008

Development, identification and validation of a mathematical model of anaerobic digestion of sewage sludge focusing on H_2S formation and transfer

F. Carrera-Chapela[a,b,*], A. Donoso-Bravo[b,c], D. Jeison[c,d], I. Díaz[e], J. A. Gonzalez[a], G. Ruiz-Filippi[b,c]

[a] *Department of Chemical Engineering, School of Engineering,University of Santiago de Compostela, Rúa Lope Gómez de Marzoa s/n, 15782 Santiago de Compostela. Spain.*
[b] *Escuela de Ingeniería Bioquímica, Pontificia Universidad Católica de Valparaíso. General Cruz 34, Valparaíso, Chile.*
[c] *INRIA-Chile. Communication and Information Research and Innovation Center (CIRIC), Avenida Apoquindo 2827, Piso 12, Las Condes, Santiago, Chile.*
[d] *Chemical Engineering Department, Universidad de La Frontera, Av. Francisco Salazar 0145, Temuco, Chile*
[e] *Department of Chemical Engineering and Environmental Technology, Escuela de Ingenierías Industriales, Sede Dr. Mergelina, University of Valladolid, Dr. Mergelina s/n, 47011 Valladolid, Spain.*

Abstract

At present there are plenty of models of the anaerobic digestion process; however, the impact of this odor emission on these models has received very little attention. Hydrogen sulfide (H_2S) is formed by the microbial action of sulfate reducing bacteria under anaerobic conditions which has been used as an odor trace marker for odor dispersion studies. A mathematical model focusing on the H_2S generation was developed using a reduced number of parameters of five stages. The model and parameters were calibrated and validated with experimental data from two pilot scale sewage sludge treating anaerobic reactors. The development of this model is able to describe properly the dynamic behavior of this system, particularly its gas phase composition.

Keywords: Anaerobic Processes, Dynamic Modelling, Dynamic

*Corresponding author
Email address: fabio.carrera@usc.es (F. Carrera-Chapela)

Simulation, Modelling, Waste-Water Treatment, Biogas

Nomenclature

X_0 particulate organic matter ($gCODL^{-1}$)	D dilution rate (d^{-1})
S_1 soluble organic matter ($gCODL^{-1}$)	$\xi_{in,i}$ state variable value in the inlet
S_2 acetic acid equivalent ($gCODL^{-1}$)	ξ_i state variable
S_3 sulfate (mgL^{-1})	q_c molar flow CO_2 ($mmolL^{-1}d^{-1}$)
K_{s1} affinity constant of fermentative bacteria ($gCODL^{-1}$)	ρ liq-gas desorption rate ($mmolL^{-1}d^{-1}$)
K_{s2} affinity constant of methanogens ($gCODL^{-1}$)	B bicarbonate ($mmolL^{-1}$)
K_{s3} affinity constant of SRB ($gCODL^{-1}$)	IC inorganic carbon ($mmolL^{-1}$)
K_{a1} equilibrium constant H_2S ($molL^{-1}$)	Z cations ($mmolL^{-1}$)
K_j stoichiometric coefficient	$r_{i,j}$ reaction rate for state variable i
X_1 fermentative bacteria ($gCODL^{-1}$)	X_2 methanogens bacteria ($gCODL^{-1}$)
X_3 sulfate reducing bacteria (SRB) ($gCODL^{-1}$)	k_h hydrolysis coefficient (d^{-1})
μ_{m1} maximum specific rate acidogenic bacteria (d^{-1})	μ_{m3} maximum specific rate SRB (d^{-1})
μ_{m2} maximum specific rate methanogenic archaea (d^{-1})	K_H Henry constant
ρ_{a_1} acid-base equilibrium rate ($mmolL^{-1}d^{-1}$)	K_a acid-base constant ($molL^{-1}$)

1. Introduction

In bioprocesses, the application of mathematical models allows representing and predicting the systems dynamic behavior and therefore, the establishment of control strategies and operational management measures. Unfortunately and despite the significant progress of the modeling practice in anaerobic digestion (AD), a proper application of mathematical modeling for control strategies remains a complex and an unsolved issue, which is caused, among other things by the lack of reliable, informative and affordable online measurement of the state variables [1]. The anaerobic digestion model n1 (ADM1) is a widely used model in AD, which provides a good tool to illustrate the complex system behavior of the AD [2]. However, in order to represent this complexity, a high number of state variables, physicochemical and biochemical processes, and consequently a high number of parameters need to be properly identified [3]. Hence, simpler, although still mechanistic, models have been developed. Such is the case in the AM2 model developed by Bernard et al. [1] with several modifications [3, 4], which simplifies the whole anaerobic process in two stages, acidogenesis and methanogenesis. When the hydrolysis is the limiting step of the whole reaction, for instance when particulate substrates are treated, it is necessary to include the hydrolysis stage previous to the acidogenesis [5].

The main odor emissions released to the atmosphere from the operation of WWTP come from several organic gases, but they can be characterized in terms of odor nuisance produced by sulfur reduced compounds, with H_2S as the main compound [6, 7, 8, 9, 10].The H_2S generation is mainly based on the action of sulfate reducing bacteria (SRB) that compete with methanogenic archaeas for the intermediate carbon source [7, 11, 12]. However, the generation of H_2S has been barely considered when using simplified models [7, 13, 14] despite, as previously mentioned, the importance of this compound on the global performance of the sludge management and treatment system as well as odor generation in WWTP [10].

The aim of this study is to develop a simplified mathematical model for the anaerobic digestion process that takes into account the hydrolysis and sulfate reducing action for hydrogen sulfide formation such that this model can afterwards be used to assess the odor impact of the anaerobic digestion emissions. In order to do so, a thorough and novel model application procedure, which comprises of local and global sensitivity analysis, uncertainty estimation and model validation through a double cross validation step (by using the unexplored band or corridor prediction) was used.

2. Methodology

2.1. Model assumptions and considerations

A general scheme of the bioreaction pathways is shown in Figure 1. The same stoichiometry and reaction kinetics presented by Donoso-Bravo et al. [15] were used in this study but adding the sulfate reducing stage. It must be kept in mind that any model is a mathematical projection of the actual process. For this reason, some reasonable and affordable assumptions, within the scope and objective of the model application, must be done.

- There is no biomass death decay [1].
- The volatile fatty acids (VFA) are represented as acetic equivalents [1].
- Three microbial populations are involved in the hydrolysis, acidogenesis, methanogesis and sulfate reduction processes [11, 12].
- Hydrogen production/accumulation is negligible. Therefore, SRBs use the VFAs as electron donors and the sulfate as electron acceptor, instead of hydrogen, as the electron acceptor [7, 11].

- Only bicarbonate/carbon dioxide, hydrogen sulfide/bisulfide, sulfate and proton contribute to pH according to ion balance [16].
- There is no metal precipitation, such as FeS [2].
- Biogas release is carried out by the two-film theory according to the global mass transfer coefficient $K_L A$ for hydrogen sulfide and carbon dioxide, whereas methane solubilization in water is assumed to be negligible [1].

2.2. Biological Model

2.2.1. Model Scheme Description and Stoichiometry

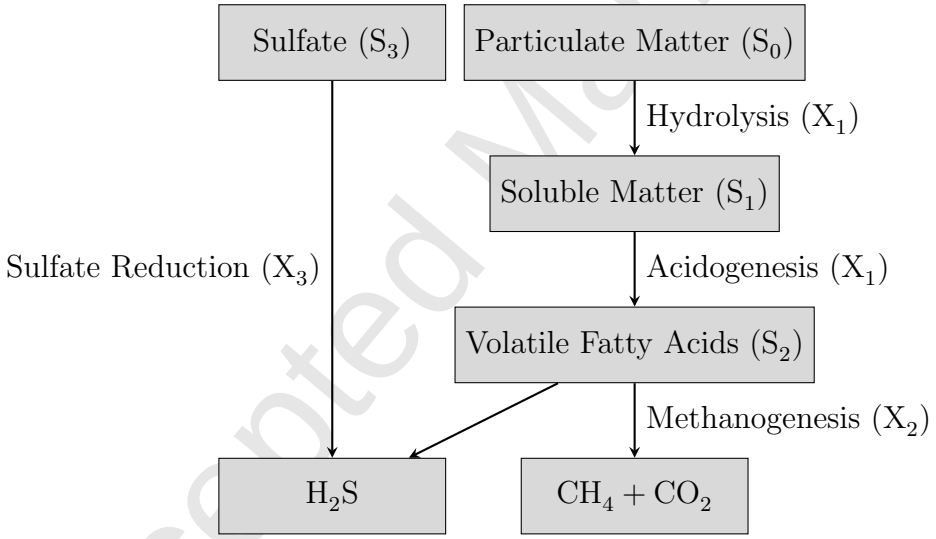

Figure 1: Scheme of the anaerobic digestion for hydrogen sulfide production.

The first stage involves the solubilization or hydrolysis of the particulate substrate. Afterwards, the soluble complex substrate is transformed into volatile fatty acids (VFA) which are represented as acetic equivalents, during the acidogenesis reaction, followed by the methanogenic step where the VFA are converted into biogas. The sulfate reduction process is carried out in parallel by the SRB using the VFA as the electron donor and the sulfate as the electron acceptor. The stoichiometric reactions considered in this model follow:

Hydrolysis:

$$S_0 \xrightarrow{r0} K_0S_1 \tag{1}$$

Acidogenesis:

$$K_1S_1 \xrightarrow{r1} X_1 + K_2S_2 + K_4CO_2 \tag{2}$$

Methanogenesis:

$$K_3S_2 \xrightarrow{r2} X_2 + K_5CO_2 + K_6CH_4 \tag{3}$$

Sulfate Reduction:

$$K_7S_3 + K_9S_2 \xrightarrow{r3} X_3 + K_{10}CO_2 + K_8H_2S \tag{4}$$

2.2.2. Model Kinetics

The hydrolysis was modeled as a Contois function because hydrolysis is considered an enzymatic reaction carried out by hydrolytic/acidogenic bacteria and assumes that a high amount of extra-cell enzyme is a consequence of an increase amount of the biomass, which leads to an increase kinetic reaction. Otherwise, the Contois function is shown to works better than classic first-order kinetics [17]. The growth function of FB and SRB bacteria are well described using the Monod kinetic, while MB can experiment uncompetitive inhibition for VFA accumulation which is best described by Haldane kinetic [1, 12]. Thus, the kinetics for specific growth rate equations FB, SRB, MB and hydrolysis are described by the following equations,

Hydrolysis:

$$r_0 = k_h \cdot \frac{S_0}{K_{s0} \cdot X_1 + S_0} \cdot X_1 \tag{5}$$

Acidogenesis:

$$r_1 = \mu_{m1} \cdot \frac{S_1}{K_{s1} + S_1} \cdot X_1 \tag{6}$$

Methanogenesis:

$$r_2 = \mu_{m2} \cdot \frac{S_2}{K_{s2} + S_2 + \frac{S_2^2}{K_{I2}}} \cdot X_2 \tag{7}$$

Sulfate Reduction:

$$r_3 = \mu_{m3} \cdot \frac{S_2 \cdot S_3}{(K_{s3} + S_2) \cdot (K_{s4} + S_3)} \cdot X_3 \tag{8}$$

2.2.3. Mass Balance

The mass balance for a continuous stirred reactor for each state variable is expressed by the following equation,

$$\frac{d\xi_i}{dt} = D \cdot (\xi_{in,i} - \xi_i) + \sum_{j=1}^{4}(K_{ij} \cdot r_j) - \rho_i \tag{9}$$

The matrix form of each term from the equation below is shown next,

$$\xi_i = \begin{pmatrix} X_1 \\ X_2 \\ X_3 \\ S_0 \\ S_1 \\ S_2 \\ S_3 \\ IC \\ H_2S \\ B \\ Z \\ H^+ \end{pmatrix} \quad ; \quad \xi_{in,i} = \begin{pmatrix} 0 \\ 0 \\ 0 \\ S_{0in} \\ S_{1in} \\ S_{2in} \\ S_{3in} \\ IC_{in} \\ 0 \\ B_{in} \\ Z_{in} \\ H^+_{in} \end{pmatrix} \quad ; \quad K_{i,j} = \begin{pmatrix} 0 & 1 & 0 & 0 \\ 0 & 0 & 1 & 0 \\ 0 & 0 & 0 & 1 \\ -1 & 0 & 0 & 0 \\ K_0 & -K_1 & 0 & 0 \\ 0 & K_2 & -K_3 & -K_9 \\ 0 & 0 & 0 & -K_7 \\ 0 & K_4 & K_5 & K_{10} \\ 0 & 0 & 0 & K_8 \\ 0 & 0 & 0 & 0 \\ 0 & 0 & 0 & 0 \\ 0 & 0 & 0 & 0 \end{pmatrix}$$

$$r_j = \begin{pmatrix} r_0 \\ r_1 \\ r_2 \\ r_3 \end{pmatrix} \quad ; \quad \rho_i = \begin{pmatrix} 0 \\ 0 \\ 0 \\ 0 \\ 0 \\ 0 \\ 0 \\ \rho_{CO_2} \\ \rho_{a_{H_2S}} - \rho_{H_2S} \\ \rho_{a_{CO_2}} \\ 0 \\ -\rho_{H^+} \end{pmatrix}$$

2.2.4. Ionic and Gaseous Compounds

The pH calculation, acid-base equilibrium for the species H_2S and CO_2 was carried out as reported by Fedorovich et al. [12], Rosen et al. [16]. The mass transfer from the liquid phase to the gas phase is modeled by the two film theory [18]. The same mass coefficient K_LA value is assumed to represent both gases since the identification of these parameters in regards to the available experimental data is not possible,

$$\rho_{\mathrm{CO_2}} = K_L A \cdot \left(\mathrm{CO_2} - K_{H_{\mathrm{CO_2}}} \cdot p_{\mathrm{CO_2}}\right) \tag{10}$$

$$\rho_{\mathrm{H_2S}} = K_L A \cdot \left(\mathrm{H_2S} - 16 \cdot K_{H_{\mathrm{H_2S}}} \cdot p_{\mathrm{H_2S}}\right) \tag{11}$$

$$\rho_{\mathrm{CH_4}} = K_L A \cdot \left(\mathrm{CH_4} - 64 \cdot K_{H_{\mathrm{CH_4}}} \cdot p_{\mathrm{CH_4}}\right) \tag{12}$$

$$\tag{13}$$

More detailed description about all differential and algebraic equations can be found in Appendix A.

2.3. Model implementation and application

Model implementation, parameter identification, calibration and validation was carried out by a systematic procedure in order to obtain reliable model response and parameter uncertainty, based on available experimental data (Figure B.5). The software used for this purpose was Matlab 2014b © with the optimization toolbox. The differential equations were solved ode23s that is based on a modified Rosenbrock formula of order 2 [19].

2.3.1. Sensitivity and Collinearity Analysis

The first step of the systematic procedure consists of a global sensitivity analysis (GSA) using ANOVA decomposition. Sensitivity analysis distinguishes the most sensitive parameters affecting the measured variables (model outputs). GSA methods evaluate the effect of a parameter while all the other parameters are varied simultaneously, accounting for interactions between parameters without depending on the simulation of a nominal point [20]. The GSA was carried out with dynamic changes on the inlet flow and concentration, as usually operated in the CSTR. The next stage of the procedure selects the parameters that are going to be estimated. Hence, a collinearity analysis was used, which allowed the detection of the parameters with less linear dependency and/or lower eigenvalues based on their local sensitivity profile [21].

2.3.2. Optimization and Model Uncertainty

Once knowing the potential vector of parameters that may be identified based on the GSA, the parameter calibration was carried out using the normalized classical least-squares estimator to exclude the scale factor problem for variables with different magnitude order and high deviation, based on the assumption that the measurement errors have a constant standard deviation, following the expression,

$$J_{NLS}(\theta) = \sum_{t=1}^{N} \left(\frac{y_{exp} - \mu_{exp}}{\sigma_{exp}} - \frac{y_{sim}(t,\theta) - \mu_{sim}}{\sigma_{sim}} \right)^2 \tag{14}$$

where J_{LS} is the objective cost function to minimize, y_{exp} are the experimental measured data, y_{sim} are the model predicted outputs, θ represents

the parameters to be determined and N the number of measurements. The initial values of the parameters were taken from literature in order to start from a feasible real initial state point.

As important as the calibration itself, having an idea of the uncertainty of the parameters cannot be neglected. One approximation method is considered to carry out the confidence intervals: approximation of the covariance matrix throws Fisher Information Matrix [22]. This method leads to the definition of statistically significant confidence regions.

2.3.3. Prediction Corridors

In order to transfer the parameter uncertainty into the model predictions output, a random sampling of 10000 data point with specified range for each parameter according to its confidence interval and distributed uniformly using the Latin hypercube approach was performed [23]. After that, the corresponding percentiles 99 and 1 as upper and lower bounds of the models outputs were added to the simulations (prediction corridor). This bounded region allows to quantify the number of experimental data that are included in it, providing a percentage of accuracy defined as,

$$accuracy(\%) = \frac{y_b}{y_t} \cdot 100 \tag{15}$$

where, y_b number of experimental data included in the bounded prediction corridor, y_t total experimental data.

2.4. Experimental Data

The experimental data was obtained from two pilot-scale anaerobic reactors fed with mixed sludge from an urban WWTP, with a working volume of 200 L (250 L total volume) which ran in parallel with the same substrate. Reactor 1 was mixed with sludge recirculation provided by a peristaltic pump and reactor 2 was mixed with biogas recirculation provided by a compressor [24]. Table 1 shows the experimental data-sets used for calibration and validation. The main operational conditions were HRT of 20 days, $T = 35 \pm 1°C$, sludge inflow concentration range of 94-48 $g\ L^{-1}$ and concentration $NaSO_4$ inflow of 2.2 $g\ L^{-1}$. More details can be found at Díaz et al. [24]. During the sludge storage, even at low temperatures, the hydrolysis of the particulate organic matter continues. Unfortunately, daily measurements of particulate (CODp) and soluble CODs of the sewage are not usually performed due to

cost and working hours that it implies. In our case, sludge characterization was performed every 3 days. Therefore, in order to include this degradation storage effect, we proposed a factor with a value of 0.01, which reflects that because of the storage there is a 1% of solubilization every day of S_0 (CODp) into S_1 (CODs).

Table 1: Experimental data-sets used for calibration and validation.

	Calibration Data	Validation Data
Reactor 1	1 - 85	86 -136
Reactor 2	0	1-70

3. Results and discussion

3.1. Global Sensitivity Analysis

The results of the GSA shows there is a high parameter interaction (Figure 2), which is expressed as the difference between the first (blue) and the higher order indexes $S_i - S_{ti}$ (red), as a result of the high non linearity of the model. It is quite difficult to identify the optimal values of each parameter for a specific experimental data set when using non linear models due to their parameter interaction. This is due to the weak influence that each parameter, by itself, exerts upon the output variables. In other words, the variable is more influenced by the joint parameter action ($S_i - S_{ti}$) than only one parameter (S_i) [25].

The models kinetic parameters are less sensitive than its stoichiometric parameters giving it a higher first order sensitivity over kinetics. Measured variables expressed as a combination of model state variables would presumably reflect less influence on parameter estimation because, as in the case of carbon dioxide, its formation is a sum of two different state variables, the acidogenic and methanogenic biomass and the physic-chemical equilibrium liquid-gas, resulting in many factors that influence its release into the gas phase.

This type of digester operation (dynamic inlet) produces a significant perturbation of the model state variables, which leads to a higher variance of the model output and consequently, an increase in the sensitivity indexes,

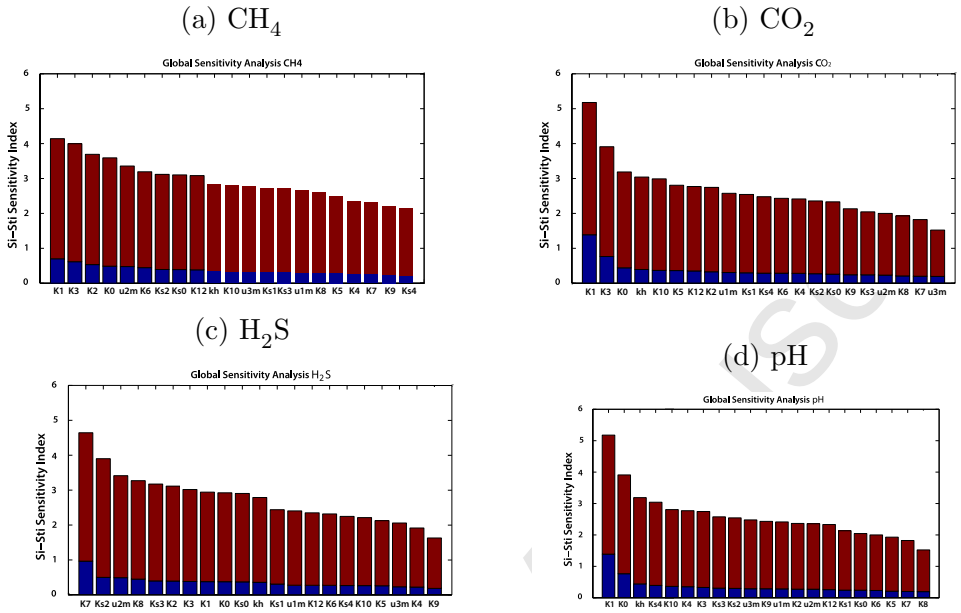

Figure 2: Global sensitivity analysis applied to measured output variables (a) CH_4, (b) CO_2, (c) H_2S and (d) pH.

since this method uses ANOVA analysis. The results of the GSA lead to establish the preliminary set of potential identifiable parameter: k_h, K_0 K_1, K_3, K_7, μ_{1m}, μ_{2m}, μ_{3m}, K_{s3}. This set presents the high sensitivity and presumable reflects higher model output perturbation and less identification uncertain.

3.2. Collinearity Analysis

The results obtained from GSA reflect that 9 parameters collect most of the variability in terms of the variance from the model outputs, these being the most sensitive parameters and, a priority, the best parameters to be identified. Nevertheless, sensitivity analysis (SA), either the global or the local approach, on its own, is not a robust methodology to select the correct parameter subset because the results can conclude that the most influential parameters can share their sensitivity profiles over time, thus, balancing out the effect of one parameter value change with the modification of other parameters. Collinearity analysis complements SA selecting those parameters whose sensitivity profiles are more independent, in other words, those subsets with the lower eigenvalues from the scaled sensitivity matrix

[21].

The results of the collinearity analysis are presented in Table 2. The parameters contained in the subset of 9 dimension are different from those obtained with GSA. The kinetic coefficients k_h, μ_{2m}, μ_{3m} and K_{s3} are now included in it. Collinearity analysis indicates that even though the other parameters present higher sensitivity indexes (Si Sti), they are linear dependent and this fact will make the parameter identification during the optimization process more complicated, with the risk of increasing the uncertainty of the optimal values.

Table 2: Subsets of parameters with the lower collinearity index value below 10.

Set	K_0	k_h	K_3	K_4	K_7	K_9	μ_{1m}	μ_{2m}	μ_{3m}	K_{s0}	K_{s1}	K_{s3}	K_{s4}	K_{12}
5			x					x	x	x			x	
6	x				x			x		x			x	x
7	x					x	x			x			x	x
8			x	x		x		x		x	x	x	x	
9		x		x		x		x	x	x	x	x		x

The parameters subset selected to carry out the calibration was chosen while taking into account GSA and collinearity results, because none of them on their own can provide sufficient information about the best parameter subset to be identified. The procedure to select the parameter subset is, first of all, to present enough sensitivity in regards to the experimental data, and to use a parameter subset with a collinearity index below 10 and not necessarily the lower of this subset dimension [21].

For this reason the parameter subset used for the calibration comprises the parameters with high sensitivity indexes (global and local) and low linear dependency ($\gamma_k = 8.7$). The chosen subset is shown next:

$$\hat{\Theta} = \{k_h, K_1, K_2, K_6, K_7, K_{10}, \mu_{2m}, \mu_{3m}, K_{s3}\} \tag{16}$$

3.3. Model Calibration-Validation

The calibration of the model was carried out using the experimental data from the reactor 1 taken from Díaz et al. [24] by using the first 85 of the 136 days of operation (Figure 3). The first cross validation was performed with the rest of the data (Table 1). The simulation results are depicted along with their respective prediction corridor.

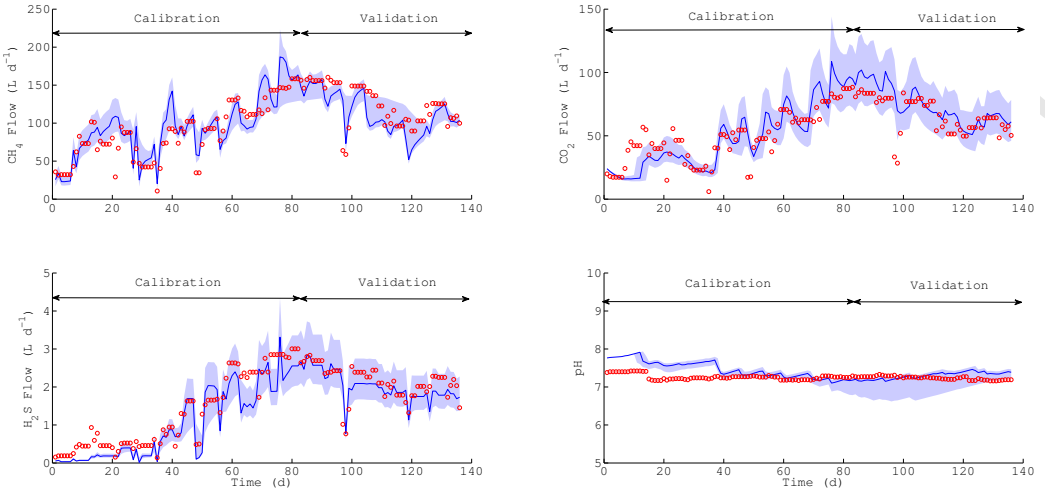

Figure 3: Calibration-validation of the model parameters for the measured data CH_4, CO_2, H_2S and pH with the predicted corridor bands with 99 of confidence.

First off, the models ability of predicting the experimental values can be seen. The models sound response to several spikes and drops of the measured outputs is worth noting, especially for CH_4 and H_2S. The CO_2 prediction is also quite acceptable although not as good as the other gases, which may be explained due to the complexity of the CO_2s behavior in AD systems. Despite not using pH measurement for calibration purposes, the model, regardless, is able to predict close values to the experimental data for this variable.

The main disagreements of the model and the experimental data are related to some operational problems that occurred, especially in regards to pumping and mixing difficulties that are not taken into account in the models description. It is worth to keep in mind that when treating sewage sludge this kind of situations may take place regularly. Similar disturbances the model was not able to predict may be found in those studies where solid substrates have been fed to the reactor [26, 27, 28].

The models ability to predict along with predicting bands or corridors in both the calibration and validation periods, it helps to understand in a much insightful way how the uncertainty of parameter is propagated to the simulation results. To our knowledge, this is the first study that actually does something like that, which makes more sense in regards to the real capability of a mathematical model. Disagreements between the simulated values and the experimental data are always present; therefore, this procedure may

offer a clearer picture of the modeling practices benefits. Barrera et al. [14] presented an extension of the ADM1 in order to include sulfate reduction agents in a reactor treating vinasse wastewater and some deviations were particularly observed during the validation of the model for both the H_2S and the total biogas production. Despite the uncertainty, the parameters were calculated, no propagation of this into the simulation was shown.

The calibrated values of the parameters are presented in Table 3. The results of the calibration are quite different from the reference-initial values. The hydrolysis constant is lower than the value reported by Donoso-Bravo et al. [15] but very similar to Vavilin et al. [5]. The hydrolysis constant calibrated is closer to the reported values for the primary sludge than the secondary sludge, which points out that the properties of mixed sludge are mostly influenced by the presence of primary fresh sludge than secondary sludge, which degradation is slower. The affinity coefficient of the SRB for the H_2S formation is considerably higher than that estimated by Fedorovich et al. [12], but this could be the result of considering all VFA as acetic acid in our model, grouping on this state variable other bacteria groups, resulting on an apparent affinity constant responsible for sulfate consumption. On the other hand, the stoichiometric coefficient responsible for methane formation is lower and the VFA generation from acidogenesis is higher than the reference values but this result could be explained because the microbial community and its pathways represented in the model differs from the reference models.

Table 3: Calibrated model parameters values obtained from the experimental data of reactor 1 with their confidence interval (CI) [24].

Parameter	Calibrated Value (CI)	Reference Value (CI)	Author
k_h	1.6 $\pm$(2.7)	6	[15]
K_1	68 $\pm$(21)	42.14 $\pm$18.94	[1]
K_2	269 $\pm$(89)	116.5 $\pm$113.6	[1]
K_6	40 $\pm$(6)	453 $\pm$91	[1]
K_7	0.734 $\pm$(0.097)	0.362 $\pm$91	[12]
K_{10}	10 $\pm$(2)	-	New parameter
μ_{2m}	0.30 $\pm$(0.05)	0.74 $\pm$0.9	[1]
μ_{3m}	0.79 $\pm$(2.19)	1.03	[12]
K_{s3}	0.55 $\pm$(0.52)	10^{-4}	[12]

The confidence intervals for each parameters are in the same order of

magnitude from reported reference values. Kinetic parameters present a higher uncertainty on their identification than the stoichiometric in regards to the available experimental data set. Parameter uncertainty is related with the available measurements and the operational conditions which did not change significantly throughout the reactors operation. One interesting operational strategy is to perform substrate pulses (VFA for example), this minimizes the lack of input excitation of many state variables which of course influences the parameters identification [29]. Zonta et al. [25] explained that parameter identification is strongly dependent on the quality and variability of the experimental data set being used. The accuracy of the prediction for gas phase composition presented an accuracy of 90%, for hydrogen sulfide and carbon dioxide, and 60% for methane, within 99% of confidence.

3.4. Second model cross validation

When cross-validation is carried out, it is usually done only with data from the same reactor operating at different operational conditions. In this case, we tested the model with data from another reactor inoculated with the same anaerobic sludge, which means that the identified parameters for the first reactor should be approximately the same, such that the model must yield similar prediction results (Figure 4). The behavior of the pH has the same pattern than the previous calibration-validation, close to the simulated (± 0.5 and $R = 0.27$) and the measured values. The model overestimates the pH value, pointing out the lack of information on the ion balance measurements, e.g. partial alkalinity, in order to improve this issue. pH is often a complicated variable to predict well because of the fact that a logarithmic expression is responsible for its calculation such that that a slight change of any of ion present in the system may lead to a significant drop or raise of the pH value.

The prediction of the methane flow throughout the whole period, except for some points at the beginning of the reactor operation, is quite good, which means that the parameter values estimated with the other reactor holds for this reactor as well.

The difference between the predicted and measured carbon dioxide flow in reactor 2 could be given by the distinct mixing mechanism used on this system (sludge recirculation instead of biogas). During the biogas injection for mixing, the gases contained in the gas phase are bubbled in the liquid phase and promotes solubilization. Because of that, the deviation from reactor 1 and 2 in the gas phase appears in both figures. As in the previous case,

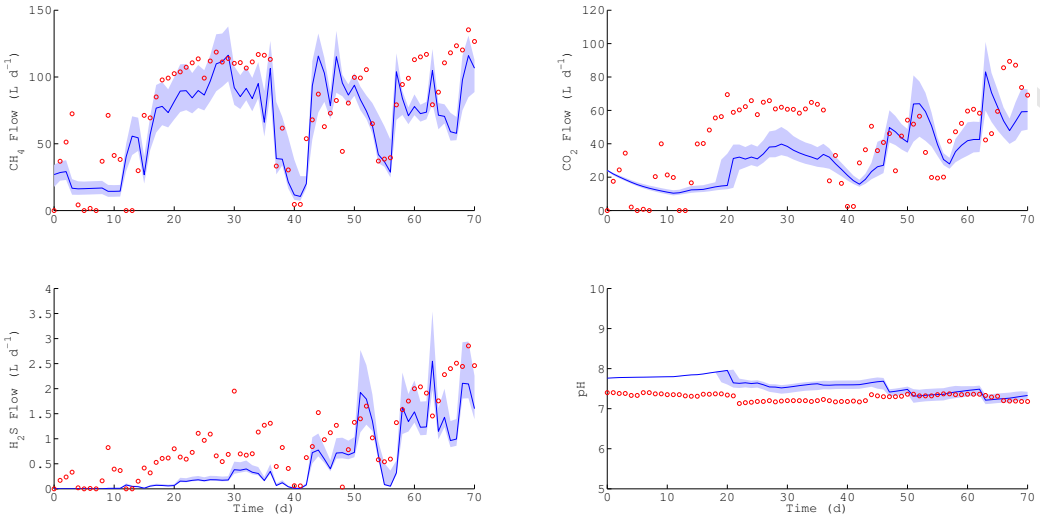

Figure 4: Validation of the model parameters for the measured data CH_4, CO_2, H_2S and pH using the reactor 2 mixed by biogas injection with the predicted corridor bands with 99 of confidence.

the H_2S generation shows the best fit with the highest correlation coefficient.

4. Conclusions

A simplified mechanistic model to predict the H_2S production from anaerobic sludge digestion of an urban wastewater treatment plant was implemented and validated with two pilot scale CSTR systems treating sewage sludge. In order to count with a proper model, implementing a procedure that comprises of local and global sensitivity analysis, uncertainty estimation and the parameters as well as uncertainty propagation on the model outputs was applied. This model may now be used to establish corrective actions to manage odor generation from anaerobic digestion and its fugitive emissions on the piping system.

5. Acknowledgments

This paper/work was partially supported by CONICYT PAI/ Concurso Nacional Tesis de Doctorado en la Empresa, convocatoria 2014, 781413011 and CIRIC - INRIA-Chile (EP BIONATURE) through Innova Chile Project Code: 10CE11-9157.

6. References

[1] O. Bernard, M. Polit, Z. Hadj-Sadok, M. Pengov, D. Dochain, M. Estaben, P. Labat, Advanced monitoring and control of anaerobic wastewater treatment plants: software sensors and controllers for an anaerobic digester., Water Sci. Technol. 43 (2001) 175–82.

[2] D. J. Batstone, J. Keller, I. Angelidaki, S. V. Kalyuzhnyi, S. G. Pavlostathis, A. Rozzi, W. T. M. Sanders, H. Siegrist, V. a. Vavilin, The IWA Anaerobic Digestion Model No 1 (ADM1)., Water Sci. Technol. 45 (2002) 65–73.

[3] S. Hassam, E. Ficara, a. Leva, J. Harmand, A generic and systematic procedure to derive a simplified model from the Anaerobic Digestion Model No. 1 (ADM1), Biochem. Eng. J. 1 (2015).

[4] A. Donoso-Bravo, J. Mailier, C. Martin, J. Rodríguez, C. A. Aceves-Lara, A. Vande Wouwer, Model selection, identification and validation in anaerobic digestion: a review., Water Res. 45 (2011) 5347–64.

[5] V. a. Vavilin, B. Fernandez, J. Palatsi, X. Flotats, Hydrolysis kinetics in anaerobic degradation of particulate organic material: an overview., Waste manage. 28 (2008) 939–51.

[6] M. Al-Shammiri, Hydrogen sulfide emission from the Ardiyah sewage treatment plant in Kuwait, Desalination 170 (2004) 1–13.

[7] W. Parker, G.-H. Wu, Modifying ADM1 to include formation and emission of odourants, Water Sci. Technol. 54 (2006) 111.

[8] F. Llavador Colomer, H. Espinós Morató, E. Mantilla Iglesias, Estimation of hydrogen sulfide emission rates at several wastewater treatment plants through experimental concentration measurements and dispersion modeling, J Air. Waste Manage. 62 (2012) 758–766.

[9] B. Wang, E. C. Sivret, G. Parcsi, X. Wang, N. M. Le, S. Kenny, H. Bustamante, R. M. Stuetz, Is H2S a suitable process indicator for odour abatement performance of sewer odours?, Water Sci. Technol. 69 (2014) 92–8.

[10] F. Carrera-Chapela, A. Donoso-Bravo, J. a. Souto, G. Ruiz-Filippi, Modeling the Odor Generation in WWTP: An Integrated Approach Review, Water Air Soil Poll. 225 (2014) 1–15.

[11] S. Kalyuzhnyi, V. Fedorovich, P. Lens, L. Hulshoff Pol, G. Lettinga, Mathematical modelling as a tool to study population dynamics between sulfate reducing and methanogenic bacteria., Biodegradation 9 (1998) 187–99.

[12] V. Fedorovich, P. Lens, S. Kalyuzhnyi, Extension of Anaerobic Digestion Model No. 1 with processes of sulfate reduction., Appl. Biochem. Biotech. 109 (2003) 33–45.

[13] I. Angelidaki, L. Ellegaard, B. Ahring, A comprehensive model of anaerobic bioconversion of complex substrates to biogas, Biotechnol. Bioeng. 63 (1999) 363–72.

[14] E. L. Barrera, H. Spanjers, K. Solon, Y. Amerlinck, I. Nopens, J. Dewulf, Modeling the anaerobic digestion of cane-molasses vinasse: extension of the Anaerobic Digestion Model No. 1 (ADM1) with sulfate reduction for a very high strength and sulfate rich wastewater, Water Res. 71 (2014) 42–54.

[15] A. Donoso-Bravo, C. Retamal, M. Carballa, G. Ruiz-Filippi, R. Chamy, Influence of temperature on the hydrolysis, acidogenesis and methanogenesis in mesophilic anaerobic digestion: parameter identification and modeling application., Water Sci. Technol. 60 (2009) 9–17.

[16] C. Rosen, D. Vrecko, K. V. Gernaey, M. N. Pons, U. Jeppsson, Implementing ADM1 for plant-wide benchmark simulations in Matlab/Simulink., Water Sci. Technol. 54 (2006) 11–9.

[17] I. Ramirez, A. Mottet, H. Carrère, S. Déléris, F. Vedrenne, J.-P. Steyer, Modified ADM1 disintegration/hydrolysis structures for modeling batch thermophilic anaerobic digestion of thermally pretreated waste activated sludge., Water Res. 43 (2009) 3479–92.

[18] R. E. Treybal, Mass-Transfer Operations, 3rd Edition, 3rd ed., McGraw-Hill Book Company, 1980.

[19] L. F. Shampine, M. W. Reichel, The MATLAB ODE Suite, Siam J. Sci. Comput. 18 (1997) 1–22.

[20] A. Saltelli, P. Annoni, I. Azzini, F. Campolongo, M. Ratto, S. Tarantola, Variance based sensitivity analysis of model output. Design and estimator for the total sensitivity index, Comput. Phys. Commun.Computer Physics Communications 181 (2010) 259–270.

[21] R. Brun, P. Reichert, Practical identifiability analysis of large environmental simulation, Water Resour. Res. 37 (2001) 1015–1030.

[22] S. Marsili-Libelli, S. Guerrizio, N. Checchi, Confidence regions of estimated parameters for ecological systems, Ecol. Model. 165 (2003) 127–146.

[23] J. L. Deutsch, C. V. Deutsch, Latin hypercube sampling with multidimensional uniformity, J. Stat. Plan. Infer. 142 (2012) 763–772.

[24] I. Díaz, S. I. Pérez, E. M. Ferrero, M. Fdz-Polanco, Effect of oxygen dosing point and mixing on the microaerobic removal of hydrogen sulphide in sludge digesters., Bioresource Technol. 102 (2011) 3768–75.

[25] Z. Zonta, M. M. Alves, X. Flotats, J. Palatsi, Modelling inhibitory effects of long chain fatty acids in the anaerobic digestion process., Water Res. 47 (2013) 1369–80.

[26] M. Lübken, K. Koch, T. Gehring, H. Horn, M. Wichern, Parameter estimation and long-term process simulation of a biogas reactor operated under trace elements limitation, Appl. Energ. 142 (2015) 352–360.

[27] U. G. Ozkan-Yucel, C. F. Gökçay, Application of ADM1 model to a full-scale anaerobic digester under dynamic organic loading conditions., Environ. Technol. 31 (2010) 633–640.

[28] X.-S. Shi, X.-Z. Yuan, Y.-P. Wang, S.-J. Zeng, Y.-L. Qiu, R.-B. Guo, L.-S. Wang, Modeling of the methane production and pH value during the anaerobic co-digestion of dairy manure and spent mushroom substrate, Chem. Eng. J. 244 (2014) 258–263.

[29] D. J. Batstone, P. F. Pind, I. Angelidaki, Kinetics of thermophilic, anaerobic oxidation of straight and branched chain butyrate and valerate., Biotechnol. Bioeng. 84 (2003) 195–204.

Appendix A. Governing Equations

Biomass:

$$\frac{dX_1}{dt} = D \cdot (X_{1_{in}} - X_1) + \mu_1(S_1) \cdot X_1 \tag{A.1}$$
$$\frac{dX_2}{dt} = D \cdot (X_{2_{in}} - X_2) + \mu_2(S_2) \cdot X_2 \tag{A.2}$$
$$\frac{dX_3}{dt} = D \cdot (X_{3_{in}} - X_3) + \mu_3(S_2, S_3) \cdot X_3 \tag{A.3}$$

Substrates:

$$\frac{dS_0}{dt} = D \cdot (S_{0_{in}} - S_0) - \mu_0(S_0, X_1) \cdot X_1 \tag{A.4}$$
$$\frac{dS_1}{dt} = D \cdot (S_{1_{in}} - S_1) + K_0 \cdot \mu_0(S_0, X_1) \cdot X_1 - K_1 \cdot \mu_1(S_1) \cdot X_1 \tag{A.5}$$
$$\frac{dS_2}{dt} = D \cdot (S_{2_{in}} - S_2) + K_2 \cdot \mu_1(S_1) \cdot X_1 - K_3 \cdot \mu_2(S_2) \cdot X_2 \tag{A.6}$$
$$\frac{dS_3}{dt} = D \cdot (S_{3_{in}} - S_3) - K_7 \cdot \mu_3(S_2, S_3) \cdot X_3 \tag{A.7}$$
$$\tag{A.8}$$

Kinetics:

Hydrolysis:

$$r_0 = \mu_0(S_0, X_1) \cdot X_1 = k_h \cdot \frac{S_0}{K_{s0} \cdot X_1 + S_0} \cdot X_1 \tag{A.9}$$

Acidogenesis:

$$r_1 = \mu_1(S_1) \cdot X_1 = \mu_{m1} \cdot \frac{S_1}{K_{s1} + S_1} \cdot X_1 \tag{A.10}$$

Methanogenesis:

$$r_2 = \mu_2(S_2) \cdot X_2 = \mu_{m2} \cdot \frac{S_2}{K_{s2} + S_2 + \frac{S_2^2}{K_{I2}}} \cdot X_2 \tag{A.11}$$

Sulfate Reduction:

$$r_3 = \mu_3(S_2, S_3) \cdot X_3 = \mu_{m3} \cdot \frac{S_2 \cdot S_3}{(K_{s3} + S_2) \cdot (K_{s4} + S_3)} \cdot X_3 \tag{A.12}$$

Ionic species:

$$\frac{dIC}{dt} = D \cdot (IC_{in} - IC) + K_4 \cdot \mu_1(S_1) \cdot X_1 + K_5 \cdot \mu_2(S_2) \cdot X_2 + \tag{A.13}$$

$$+ K_{10} \cdot \mu_3(S_2, S_3) \cdot X_3 - \rho_{\mathrm{CO}_2} \tag{A.14}$$

$$\frac{dB}{dt} = D \cdot (B_{in} - B) - \rho_{a_{\mathrm{CO}_2}} \tag{A.15}$$

$$\frac{dZ}{dt} = D \cdot (Z_{in} - Z) \tag{A.16}$$

$$\frac{d\mathrm{H_2S}_{aq}}{dt} = D \cdot (\mathrm{H_2S}_{aq_{in}} - \mathrm{H_2S}) + K_8 \cdot \mu_3(S_2, S_3) \cdot X_3 - \rho_{a_{\mathrm{H_2S}}} - \rho_{\mathrm{H_2S}} \tag{A.17}$$

$$\frac{dH^+}{dt} = D \cdot (H^+_{in} - H^+) - \rho_{H^+} \tag{A.18}$$

Algebraic equations:

$$\alpha = \frac{1}{1 + 10^{-pH + pKa_{\mathrm{H_2S}}}} \tag{A.19}$$

$$\mathrm{HS^-} = \alpha \cdot \mathrm{H_2S} \cdot \frac{33}{34} \tag{A.20}$$

$$\phi = Z - S_2 - B - \mathrm{HS^-} - S_3 \tag{A.21}$$

$$H^+ = -\frac{\phi}{2} + \frac{\sqrt{\phi^2 + 4 \cdot 1 \cdot 10^{-14}}}{2} \tag{A.22}$$

$$\rho_{a_{\mathrm{CO_2}}} = 10^{14} \cdot \left((IC - B) \cdot (Ka_{\mathrm{CO_2}} + H^+) - (Ka_{\mathrm{CO_2}} \cdot B)\right) \tag{A.23}$$

$$\rho_{a_{\mathrm{H_2S}}} = 10^{14} \cdot \left(\mathrm{HS^-} \cdot (Ka_{\mathrm{H_2S}} + H^+) - (Ka_{\mathrm{H_2S}} \cdot \mathrm{H_2S})\right) \tag{A.24}$$

$$\rho_{\mathrm{CO_2}} = K_L A \cdot \left((IC - B) - K_{H_{\mathrm{CO_2}}} \cdot p_{\mathrm{CO_2}}\right) = \tag{A.25}$$

$$= K_L A \cdot \left(\mathrm{CO_2} - K_{H_{\mathrm{CO_2}}} \cdot p_{\mathrm{CO_2}}\right) \tag{A.26}$$

$$\rho_{\mathrm{H_2S}} = K_L A \cdot \left(\mathrm{H_2S} - 16 \cdot K_{H_{\mathrm{H_2S}}} \cdot p_{\mathrm{H_2S}}\right) \tag{A.27}$$

$$\rho_{\mathrm{CH_4}} = K_L A \cdot \left(\mathrm{CH_4} - 64 \cdot K_{H_{\mathrm{CH_4}}} \cdot p_{\mathrm{CH_4}}\right) \tag{A.28}$$

$$\tag{A.29}$$

Gaseous species:

$$p_{\mathrm{CO_2}} = \mathrm{CO_2} \cdot R \cdot T \tag{A.30}$$

$$p_{\mathrm{H_2S}} = \mathrm{H_2S} \cdot R \cdot T/16 \tag{A.31}$$

$$p_{\mathrm{CH_4}} = \mathrm{CH_4} \cdot R * T/64 \tag{A.32}$$

$$p_{gas} = p_{\mathrm{CO_2}} + p_{\mathrm{CH_4}} + p_{\mathrm{H_2S}} + p_{\mathrm{H_2O}} \tag{A.33}$$

$$q_{gas} = 5 \cdot 10^4 \cdot (p_{gas} - P_{atm}) \cdot \frac{p_{gas}}{P_{atm}} \tag{A.34}$$

$$\frac{d\mathrm{CO_2}}{dt} = -\,p_{\mathrm{CO_2}} \cdot \frac{q_{gas}}{V_{gas}} + \rho_{\mathrm{CO_2}} \cdot \frac{V_{liq}}{V_{gas}} \tag{A.35}$$

$$\frac{d\mathrm{H_2S}}{dt} = -\,p_{\mathrm{H_2S}} \cdot \frac{q_{gas}}{V_{gas}} + \rho_{\mathrm{H_2S}} \cdot \frac{V_{liq}}{V_{gas}} \tag{A.36}$$

$$\frac{d\mathrm{CH_4}}{dt} = -\,p_{\mathrm{CH_4}} \cdot \frac{q_{gas}}{V_{gas}} + \rho_{\mathrm{CH_4}} \cdot \frac{V_{liq}}{V_{gas}} \tag{A.37}$$

$$\tag{A.38}$$

Appendix B. Systematic modeling procedure

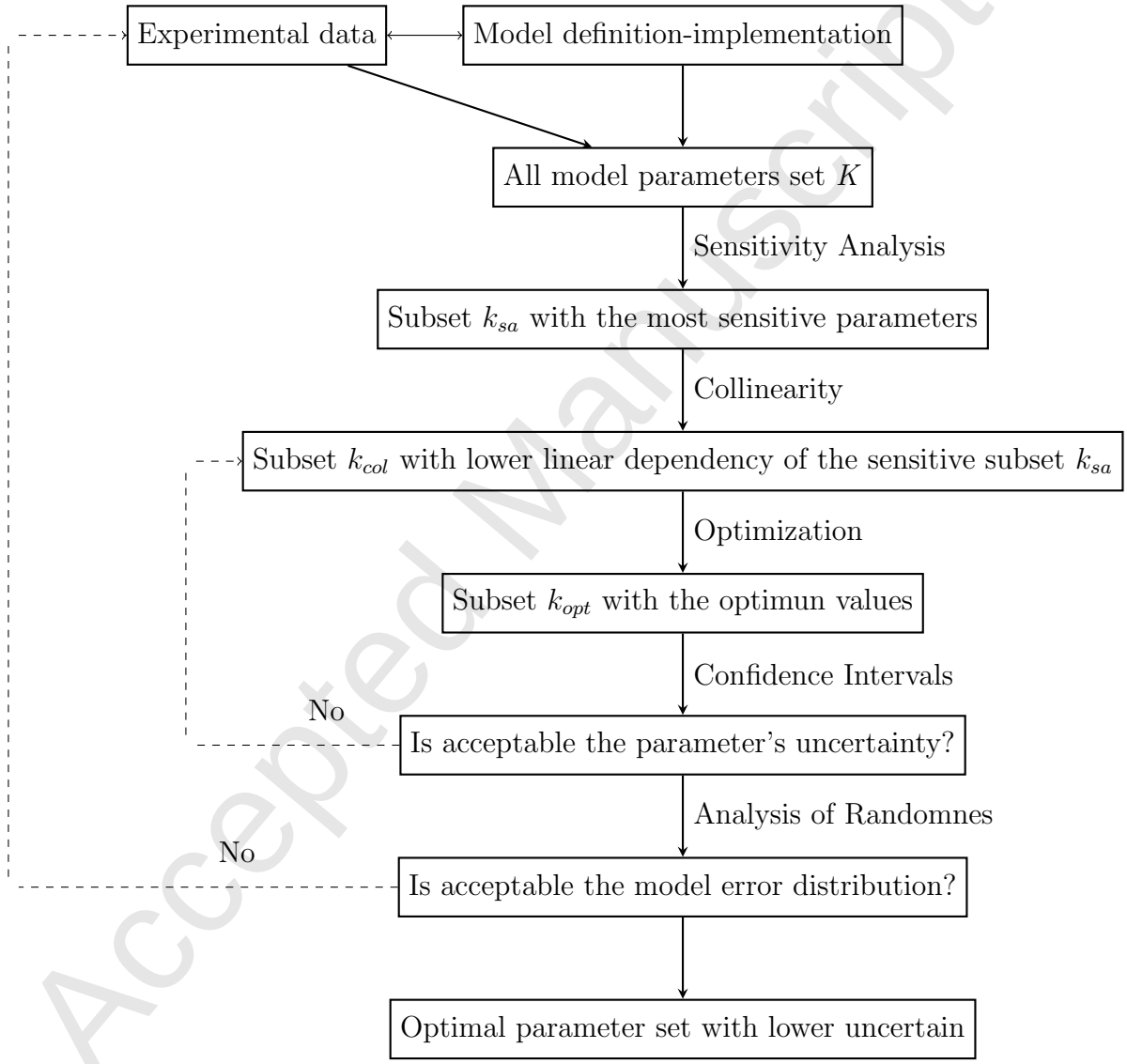

Figure B.5: Systematic procedure applied for model implementation, calibration and validation.